ABT-751, a novel tubulin-binding agent, decreases tumor perfusion and disrupts tumor vasculature

Yanping Luo, Vincent P. Hradil, David J. Frost, Saul H. Rosenberg, Gary B. Gordon, Sherry J. Morgan, Gerard D. Gagne, Bryan F. Cox, Stephen K. Tahir and Gerard B. Fox

ABT-751 is an orally bioavailable tubulin-binding agent that is currently under clinical development for cancer treatment. In preclinical studies, ABT-751 showed antitumor activity against a broad spectrum of tumor lines including those resistant to conventional chemotherapies. In this study, we investigated the antivascular properties of ABT-751 in a rat subcutaneous tumor model using dynamic contrast-enhanced magnetic resonance imaging. A single dose of ABT-751 (30 mg/kg, intravenously) induced a rapid, transient reduction in tumor perfusion. After 1 h, tumor perfusion decreased by 57% before recovering to near pretreatment levels within 6 h. In contrast, ABT-751 produced little change in muscle perfusion at either time point. To further elucidate mechanisms of drug action at the cellular level, we examined the effects of ABT-751 on endothelial cells using an in-vitro assay. ABT-751, at concentrations corresponding to plasma levels achieved *in vivo*, caused endothelial cell retraction and significant loss of microtubules within 1 h. The severity of these morphological changes was dose-dependent but reversible within 6 h after the discontinuation of the drug. Taken together, these results show that ABT-751 is a tubulin-binding agent with antivascular properties. Microtubule disruption and morphological changes in vascular endothelial cells may be responsible, at least in part, for the dysfunction of tumor blood vessels after ABT-751 treatment. *Anti-Cancer Drugs* 20:483–492 © 2009 Wolters Kluwer Health | Lippincott Williams & Wilkins.

Anti-Cancer Drugs 2009, **20**:483–492

Keywords: ABT-751, dynamic contrast-enhanced magnetic resonance imaging, perfusion, rat, tumor, vascular-disrupting agent

Global Pharmaceutical Research and Development, Abbott Laboratories, Abbott Park, Illinois, USA

Correspondence to Dr Yanping Luo, PhD, Experimental Imaging, Abbott Laboratories, Department R4DF, Building AP9-1, 100 Abbott Park Road, Abbott Park, IL 60064, USA
Tel: +1 847 935 6622; fax: +1 847 938 5286; e-mail: yanping.luo@abbott.com

Stephen K. Tahir and Gerard B. Fox contributed equally to this manuscript

Received 26 November 2008 **Revised form accepted** 24 March 2009

Introduction

Solid tumors are dependent on blood vessels to provide oxygen and nutrients for growth. Consequently, several different cancer therapy strategies targeting the tumor vasculature have been developed in recent years. These include prevention of new blood vessel formation through inhibition of endothelial cell proliferation, interrupting angiogenic pathways [1–5], or disrupting the integrity and functionality of existing tumor vasculature (or so-called vascular-disrupting agents, VDAs) [6–10]. Tubulin-binding agents target dividing cells by interfering with the dynamics of tubulin, an essential protein component of microtubules. As tumor blood vessels have abundant replicating endothelial cells [11,12], this class of agents has the potential to cause significant vascular damage in tumors and thus produce vascular-mediated cell death. In this regard, tubulin-binding agents, such as vinca alkaloids and colchicines, have shown activities to cause tumor blood flow shutdown leading to tumor necrosis, yet only at doses approaching the maximum tolerable dose (MTD) [13,14]. Novel tubulin-binding agents, such as combretastatin A-4 (zybrestat), ZD6126, and AVE8062, exhibit similar effects at doses much lower than the MTD [9,15–20], thereby offering potential for an improved therapeutic window for vascular-mediated therapeutic efficacy.

ABT-751 (formerly known as E7010; Eisai Co. Ltd., Tokyo, Japan) is a novel, orally bioavailable antimitotic agent that binds to the colchicine site on β-tubulin and inhibits microtubule formation [21]. This interference with normal microtubule dynamics leads to cell cycle arrest and cell death by apoptosis. In preclincal studies, ABT-751 has shown potent antitumor activity against a broad spectrum of murine tumors and human xenografts including colon, lung, breast, and gastric cancers [22,23]. ABT-751 is also active against a number of tumors that are resistant to vincristine or paclitaxel because of the overexpression of P-glycoprotein [21,22,24]. Furthermore, in phase 1 clinical trials, ABT-751 shows excellent oral bioavailability and achieves concentrations shown to be efficacious in preclinical models at tolerable doses [25–27].

The cytotoxic antitumor activities of ABT-751 are well characterized [21–23,28,29]. However, the dynamics of

0959-4973 DOI: 10.1097/CAD.0b013e32832c0acf

potential antivascular effects of this drug have not been explored extensively [30,31]. In the current studies, we used dynamic contrast-enhanced magnetic resonance imaging (DCE-MRI) to characterize the time-dependent in-vivo vascular response of ABT-751 in a rat subcutaneous tumor model. DCE-MRI is a noninvasive method that provides quantitative endpoint measurements of vascular function by measuring the uptake of intravenously administered contrast agent, allowing longitudinal assessment of blood vessel function [32–37]. The method offers a translational imaging tool that has been adopted in both preclinical and clinical studies to assess treatment response of antivascular agents [34–36,38]. To better understand the potential mechanisms underlying in-vivo DCE-MRI changes observed after treatment, the direct effects of ABT-751 on endothelial cells *in vitro* were investigated using a treatment protocol mimicking exposures in DCE-MRI in-vivo experiments.

Materials and methods

Animal care

Adult female Fisher 334 rats (150–160 g) were purchased from Charles River Laboratories (Kingston, New York, USA) and maintained in a temperature-controlled room on standard sterile wood chip bedding in a quiet room under conditions of 12 h lights on/12 h lights off (lights on at 06 : 00). Food and water were available *ad libitum*. Experimental protocols for all studies were approved and closely monitored by the Abbott Institutional Animal Care and Use Committee, adhering to the National Institutes of Health Guide for Care and Use of Laboratory Animals guidelines in facilities accredited by the Association for the Assessment and Accreditation of Laboratory Animal Care.

Tumor inoculation, animal preparation, and treatment

Rat 9L glioma cells were kindly provided by Dr Michael Garwood (University of Minnesota, Minnesota, USA). Cells were cultured in GIBCO Dulbecco's Modified Eagle Medium (Invitrogen Corp., Carlsbad, California, USA) containing 10% fetal calf serum, 1% L-glutamine. When grown to confluence, cells were harvested and suspended in PBS at a concentration of 3×10^7 cells/ml. Under halothane anesthesia (4% induction, 1% maintenance), rats were injected with a 0.1 ml cell suspension subcutaneously into the left, upper medial, hind limb. MRI experiments were performed approximately 2 weeks after inoculation, when tumors had reached a volume of 1.0–2.0 cm^3. Rats were then randomly selected to receive ABT-751 or vehicle treatment.

Drugs

ABT-751, *N*-[2-[(4-hydroxyphenyl)amino]-3-pyridinyl]-4-methoxybenzenesulfonamide, was synthesized at Abbott laboratories (Abbott Park, Illinois, USA). The compound was dissolved in 50% D5W and 50% PEG200 (Sigma-Aldrich, St. Louis, Missouri, USA) and administered intravenously through a programmed infusion pump at a dose of 30 mg/kg (equivalent to an oral dose of 200–250 mg/kg in patients based on area under the curve (AUC) [26]) over a 15-min period. Blood samples were collected from six rats, 1 h after ABT-751 administration, to measure plasma drug levels.

Vascular effects of ABT-751 assessed by dynamic contrast-enhanced magnetic resonance imaging

Two studies were conducted to evaluate the treatment effects of ABT-751 on tissue perfusion. The first study (study I) focused on the acute vascular responses to ABT-751 with DCE-MRI measured before and 1 h after ABT-751 administration. A second study (study II) was conducted to monitor the dynamics of the vascular response by adding an additional time point at 6 h after ABT-751 administration. A pilot study was conducted before these studies to assess whether the first DCE-MRI measurement would affect the second DCE-MRI measurement when they are conducted at a 1-h interval. Experimental design encompassing all studies is detailed in Table 1.

Before MRI experiments, rats were anesthetized with a mixture of 90 mg/kg ketamine (Fort Dodge Animal Health, Fort Dodge, Iowa, USA) and 10 mg/kg xylazine (Phoenix Pharmaceuticals, St. Joseph, Missouri, USA). The tail vein and femoral vein were catheterized for contrast agent and compound administration, respectively. To evaluate animal physiological status during MRI experiments, mean arterial pressure (MAP) and heart rate (HR) were monitored in a subset of animals ($N = 8$/group) through a femoral artery catheter.

All MRI experiments were conducted on a 4.7-T/40 cm magnet (Varian Inc., Palo Alto, California, USA) with a 12-cm bore gradient insert operated by a Varian INOVA imaging console (Varian Inc., Palo Alto, California, USA). After preloading contrast agent and compound solution into the catheters, rats were placed in the supine position, with hind limbs in the center of a 6-cm quadrature volume coil. Body temperature was maintained at 37°C throughout the experiment using a blanket heated with circulating warm water. DCE-MRI was performed over a 3-mm-thick cross section of the hind limbs. A capillary phantom was used to delineate

Table 1 Study designs of DCE-MRI experiments

	Treatment	Time points of DCE-MRI	Number of animals/group
Pilot study	None	0 and 1 h	7
Study I	Vehicle or ABT-751	Before and 1 h after dosing	8
Study II	Vehicle or ABT-751	Before and 1 and 6 h after dosing	8

DCE-MRI, dynamic contrast-enhanced magnetic resonance imaging.

the imaging slice to insure that MR images acquired at different time points were from the same tissue region. Animals were allowed to recover from anesthesia with free access to food and water after MRI measurements at the 1 h time point. At 6 h post-treatment, rats were anesthetized again and prepared with a tail vein catheter for contrast agent delivery. DCE-MRI was performed over the same tissue region that was imaged earlier.

DCE-MRI was conducted using a T_1-weighted gradient echo-imaging sequence. In each DCE-MRI measurement, a total of 20 baseline images were collected before a bolus injection of the contrast agent, gadolinium diethylenetriaminepentaacetic acid (Gd-DTPA; 0.2 mmol/kg, intravenously; Bayer HealthCare Pharmaceuticals, Wayne, New Jersey, USA). Data acquisition was continued for 4 min with a time resolution of 2 s per image to monitor tissue uptake of the contrast agent. Imaging parameters were: repetition time/echo time = 30 ms/2 ms, field of view $6.4 \times 6.4\,cm^2$, imaging matrix 128×64.

Data analysis

On the basis of tracer kinetics, the initial uptake of contrast agent Gd-DTPA is flow-dependent, as tissue capillaries are highly permeable to Gd-DTPA [37]. It has been shown in myocardium, skeletal muscles, and tumors that the initial maximum slope (S_M) of the contrast enhancement curve measured by DCE-MRI correlated well with tissue blood flow, and thus can be used as a surrogate index for tissue perfusion [39–41]. Another commonly used parametric measure of initial tracer uptake is the initial AUC (IAUC), which has been adopted widely for preclinical and clinical evaluation of antivascular effect of VDAs, such as combretastatin A-4 and ZD6126 [33,35,38]. In this study, we used both indices, S_M and IAUC over the first 30 s after contrast agent injection, illustrated in Fig. 1b as surrogate evaluation of tissue perfusion.

Before imaging analysis was performed, dynamic contrast enhancement curves from each pixel were fitted with a multivariate function with three exponential terms to minimize noise contribution (solid lines in Fig. 1b–d) [40]. Both S_M and IAUC were calculated on a pixel-by-pixel basis, and then averaged over manually outlined regions of interest: muscles of two hind limbs and tumor tissue (Fig. 1a). To reduce interanimal variation, S_M and IAUC were normalized using S_M and IAUC of the nontumor-bearing limb muscle as internal references (calculated as a ratio of S_M of the region of interest over the S_M of muscle). Post-treatment-to-pretreatment ratio of these normalized indices were calculated to reflect the treatment-induced changes and presented as group mean ± SEM. Statistical comparisons between different time points and between different treatment groups were performed using two-tailed Student's *t*-tests.

Fig. 1

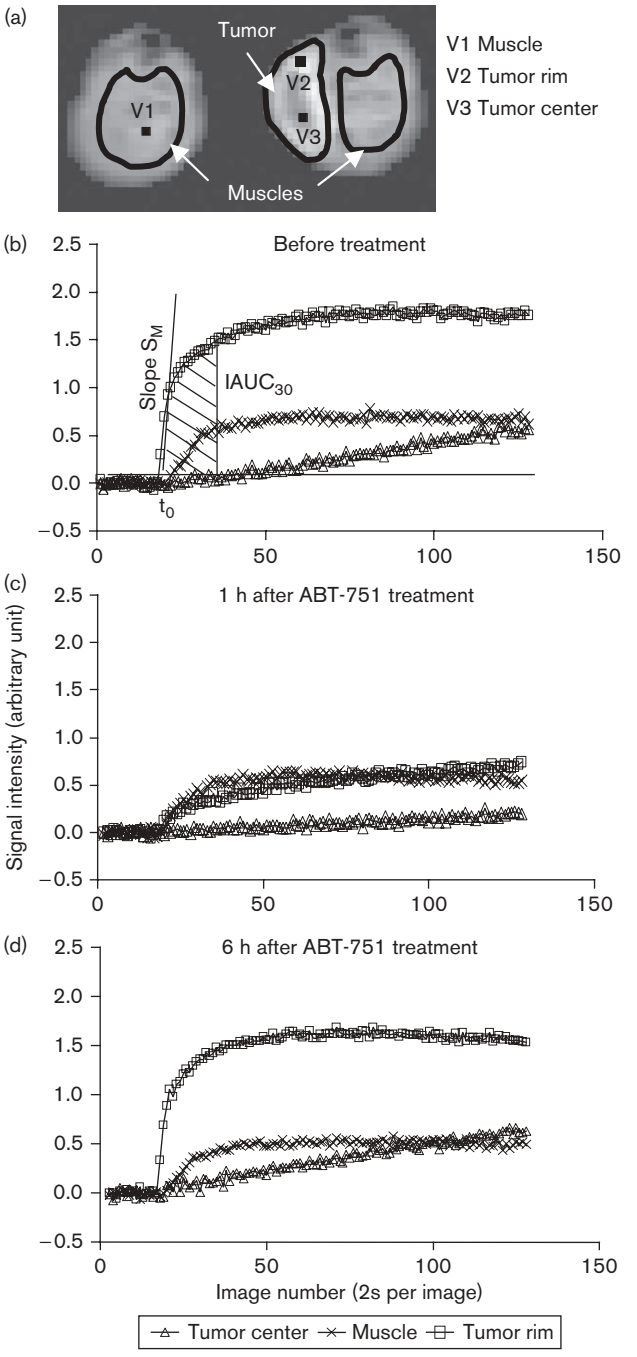

Representative dynamic contrast-enhanced magnetic resonance imaging data collected from a rat treated with ABT-751 (30 mg/kg). (a) A T_1-weighted gradient echo image from a cross-section of rat's hind limbs and a subcutaneous tumor at 50 s after contrast agent injection. Regions of interest were manually outlined over muscles of each hind limb and tumor. Muscle from nontumor-bearing limb was used as internal reference tissue. Three voxels are indicated to represent data from V1, muscle; V2, tumor rim; and V3, tumor center. Representative signal enhancement curves and the fitted ones (solid lines) from regions V1, V2, and V3 acquired (b) before treatment, (c) 1 h, and (d) 6 h after treatment are illustrated. The analysis of the signal enhancement curves is illustrated in (b), where S_M is the maximum slope of the curve and $IAUC_{30}$ is the initial area under the curve over the first 30 s after contrast injection. Time resolution for imaging acquisition is 2 s/image.

Tumor histology

After DCE-MRI at 1 h post-treatment in study I and at 6 h post-treatment in study II, tumors were excised, immersion-fixed in 10% formalin, and embedded in paraffin. From each tumor, five tissue sections of 5-μm thickness were prepared from the same tissue regions at which DCE-MRI data were acquired. These histological sections were then stained with hematoxylin and eosin for quantitative morphometric evaluation of tumor necrosis: three slides were selected for analysis based on the quality of staining. Images of whole sections were taken using a SPOT-RT digital camera (Diagnostic Instruments, Sterling Heights, Michigan, USA) mounted on a Leica MZ FLIII (Leica, Deerfield, Illinois, USA) stereomicroscope. Metamorph imaging software (Universal Imaging, Downington, Pennsylvania, USA) was used for image acquisition and processing. For each section, total tumor area (necrotic + non-necrotic area) and necrotic tumor area were detected by color thresholding and separately measured using a macro developed with the Metamorph software (Universal Imaging). Results are expressed as tumor necrotic area fraction (NAF; area of necrosis divided by the total tumor area).

In-vitro effects on endothelial cell morphology

Human dermal microvascular endothelial cells were obtained from Cambrex Bio Science Walkersville (Walkersville, Maryland, USA) and maintained in EGM-2 MV (Cambrex Bio Science Walkersville) containing 5% fetal bovine serum in a humidified chamber at 37°C

Fig. 2

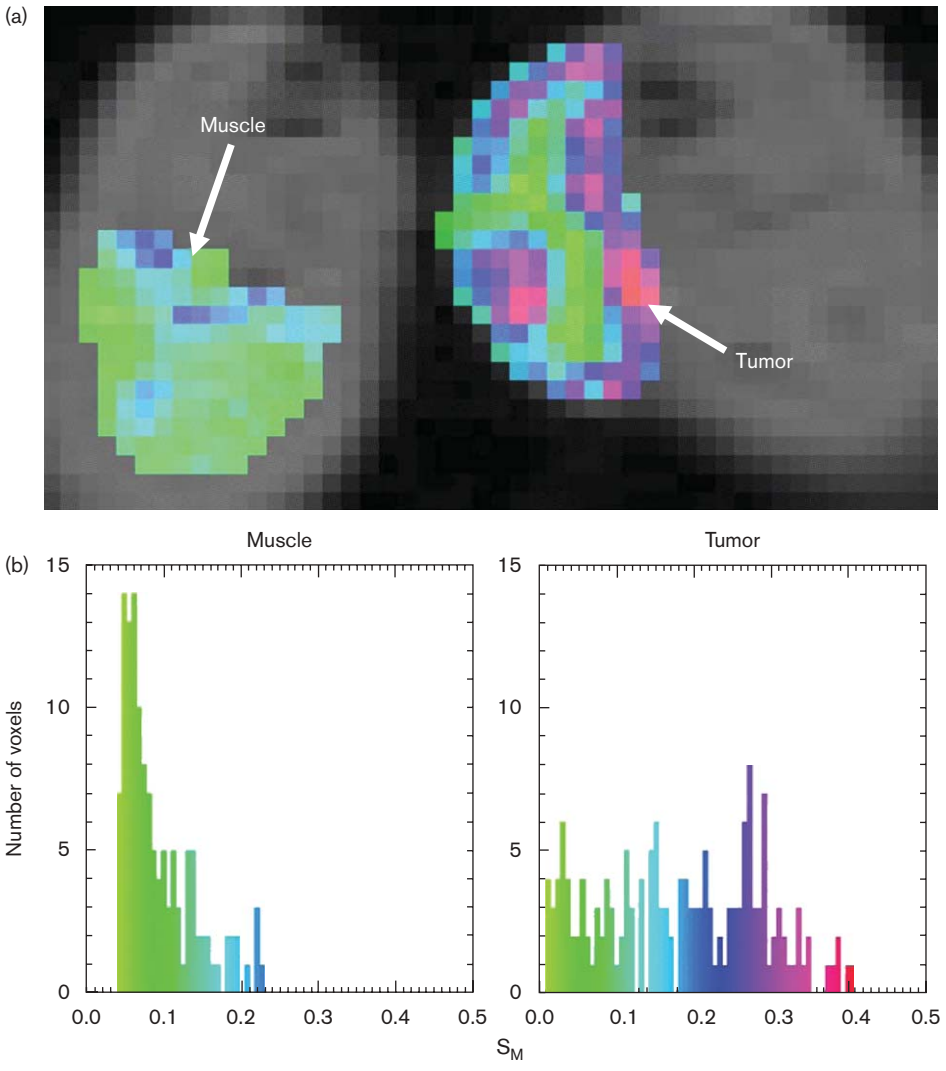

Example maximum slope (S_M) map overlaying with an anatomical MR image from a rat before treatment (a) and the corresponding color-matched histograms of S_M in tumor and muscle (b). The distribution of S_M within the tumor is highly heterogeneous, with higher values at the tumor rim and lower values toward the tumor center. In contrast, S_M in muscle tissue from hind limb is relatively homogeneous.

containing 5% CO_2. Cells were plated in eight chamber slides at 2×10^4 cells/well and allowed to attach overnight. Cells were then treated with 0.3, 1, 3, or 10 µmol/l ABT-751 for 1 h on the next day with the vehicle used as control. Changes in endothelial cell shape were examined using nonconfluent, proliferating, human dermal microvascular endothelial cells to mimic the immature vasculature of tumor vessels. After treatment, one set of cells was fixed with 10% phosphate-buffered formalin for 10 min and another set of cells was washed with PBS twice after the 1 h treatment, allowed to recover for 5 h in fresh medium, and then fixed in formalin. Fixed cells were washed once with PBS and stained for microtubules and microfilaments with fluorescein isothiocyanate-conjugated mouse antitubulin IgG (Sigma, St. Louis, Missouri, USA) and Alex Fluor 546-conjugated phalloidin (Molecular Probes, Eugene, Oregon, USA), respectively, as described earlier [42]. Cells were imaged with a Bio-Rad MRC-1000 Confocal Imaging System attached to an inverted Nikon microscope (Bio-Rad Laboratories, Hercules, California, USA) fitted with epifluorescence optics and using a 60 × objective (numerical aperture = 1.4).

Results

Pilot study

In seven tumor-bearing rats, S_{Ms} or IAUCs obtained from two consecutive DCE-MRI conducted at a 1-h interval were not statistically significant. The average percentage change of S_M was $-3 \pm 14\%$ ($P = 0.94$) and $-12 \pm 10\%$ ($P = 0.08$) in muscle and tumor, respectively, whereas the percentage change in IAUC was $-1 \pm 9\%$ ($P = 0.32$) and $0 \pm 10\%$ ($P = 0.16$) in muscle and tumor, respectively. Thus, the clearance of the contrast agent was adequate within 1 h such that the first injection had little effect on the subsequent measurements of S_M or IAUC.

Study I, II: effects of ABT-751 on maximum slope and initial area under the curve

Gross evaluation of DCE-MRI data revealed, in general, that faster signal increases and higher signal enhancement were observed in tumor tissue compared with muscle (Fig. 1b). The average S_M and IAUC in tumors were 2.6 ± 0.2 and 2.2 ± 0.1 times of those observed in muscle, respectively. The distribution of S_M and IAUC within tumors was highly heterogeneous, with higher values observed at the tumor rim and lower values at the tumor center (Fig. 2). In contrast, S_M and IAUC in muscle tissue were relatively homogeneous.

Representative signal enhancement curves acquired at 1 and 6 h post-ABT-751 administration are shown in Fig. 1c and d. Group average of treatment-induced changes in S_M and IAUC are presented using posttreatment-to-pretreatment ratios (Fig. 3). Results at the 1 h time point from study I and II were consistent with each other confirming the reproducibility of the vascular effects produced by ABT-751. On account of the consistent findings from the two studies, group means at the 1-h time point were combined and used to describe the overall results. A single dose of ABT-751 at 30 mg/kg profoundly affected tumor vessel function, causing significant reduction in S_M and IAUC in tumors. One hour after compound administration, S_M and IAUC in tumors decreased to $43 \pm 5\%$ ($P = 0.00001$) and $54 \pm 4\%$ ($P = 0.00001$) of the pretreatment values, respectively, whereas in the vehicle-treated rats, tumor S_M and IAUC were 100 ± 9 and $105 \pm 6\%$ of the pretreatment values, respectively.

Fig. 3

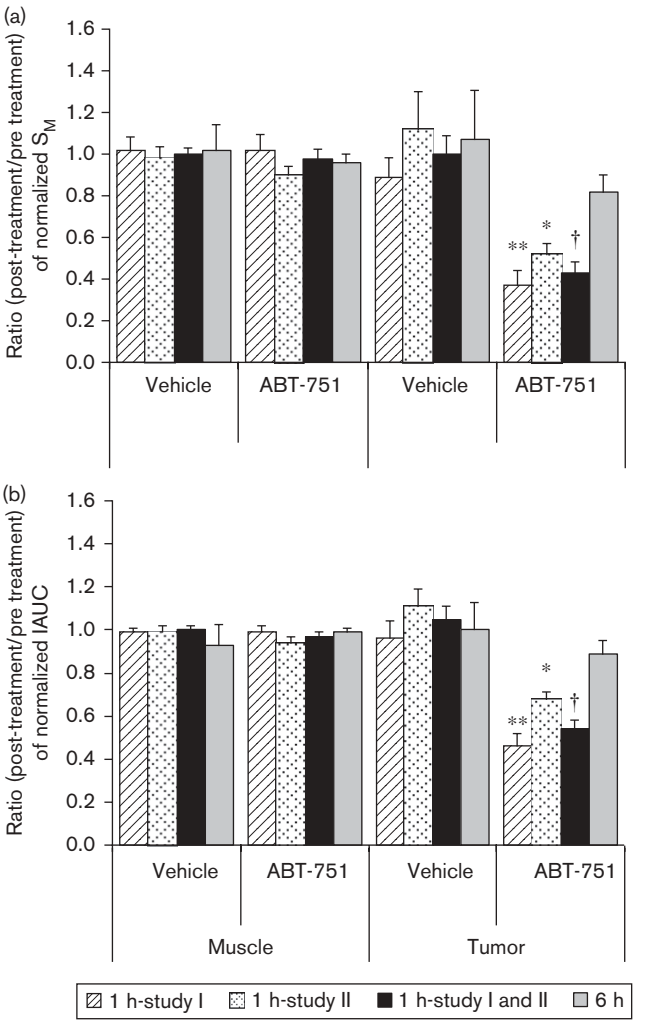

Vascular effect of a single dose ABT-751 (30 mg/kg) on normal muscle and tumor at 1 and 6 h after treatment as assessed by perfusion indices: (a) maximum slope (S_M), $^*P < 0.01$ versus vehicle, $^{**}P < 0.0003$ versus vehicle, $^{\dagger}P < 0.00001$ versus vehicle; and (b) initial area under the curve (IAUC), $^*P < 0.002$ versus vehicle, $^{**}P < 0.0002$ versus vehicle, $^{\dagger}P < 0.00001$ versus vehicle. Results are presented as mean (measured from whole tumor) ± SEM. Measurements of S_M and IAUC at 1 h are consistent in study I and II. Significant reduction in both S_M and IAUC was observed in tumor but not in hind limb muscles at 1 h post-treatment. By 6 h, both indices recovered to approximately 80–90% of the baseline level.

After decreases in tumor S_M and IAUC, recovery in both S_M and IAUC was apparent. By 6 h after treatment, S_M and IAUC in tumors increased to near pretreatment values, accounting for 82 ± 8 and $89 \pm 6\%$ of the pretreatment level, respectively. Statistically, these values were not different ($P = 0.36$ for S_M and $P = 0.16$ for IAUC) from those observed in the vehicle-treated group at 6 h. The changes in S_M and IAUC of hind limb muscles were assessed to evaluate the treatment effects on normal blood vessels. No significant treatment-induced changes in S_M or IAUC of muscle tissues were observed at either time point (Fig. 3).

To evaluate possible differential vascular effects of ABT-751 in different tumor regions, S_M was plotted as a function of the distance to tumor edges (Fig. 4). The pretreatment S_M was higher indicating a higher perfusion in the tumor rim as compared with the tumor center. This observation is consistent with general tumor biology that the tumor rim is often supplied with extension of blood vessels from surrounding normal tissues and undergoes active angiogenesis, whereas the tumor center relies on ill-formed tumor blood vessels or contains no blood vessels. S_M in all tumor regions decreased significantly 1 h after the ABT-751 administration. Although the decrease in S_M was more pronounced in the tumor rim, the S_M of tumor rim remained at a comparable level with that of normal muscle, whereas S_M in the tumor center was reduced nearly to zero. Six hours after the treatment, S_M of all tumor regions recovered significantly with more complete recovery observed in the tumor rim.

Fig. 4

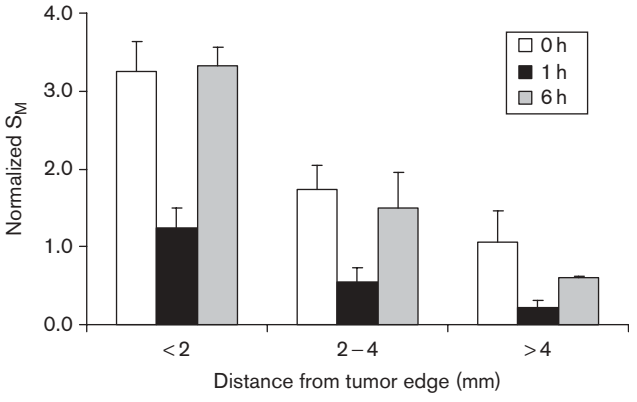

Vascular effect of a single-dose ABT-751 (30 mg/kg) in different tumor regions presented by maximum slope (S_M) as a function of the distance to tumor edge. S_M of all tumor regions was significantly reduced by ABT-751 at 1 h post-treatment and largely recovered within 6 h posttreatment.

Rat physiological conditions were monitored and maintained stable during the MRI experiments. MAP and HR recorded during the first hour after the ABT-751 infusion are presented in Table 2. A single dose of ABT-751 at 30 mg/kg did not cause significant changes either in MAP or in HR. The average plasma concentration of ABT-751 measured at 1 h after compound administration was 2.07 ± 0.77 μmol/l.

Effects on endothelial cell morphology

The direct effect of ABT-751 on endothelial cells *in vitro* was assessed using HMVECs at a concentration range of 0.3–10 μmol/l, covering the plasma drug concentrations achieved in the in-vivo experiments. HMVE control cells were well spread out on the slides and their body length was generally oriented in parallel with the other surrounding cells. Control cells had an extensive microtubule network extending out to the cell periphery and contained many prominent stress fibers extending throughout and along the length of the cell body (Fig. 5a–c). Endothelial cell retraction was observed after the treatment with 0.3 μmol/l ABT-751 (data not shown), which was associated with a decrease in microtubules in the cell periphery. After 1 h treatment with 1 μmol/l ABT-751, the cells became more retracted, there was a noticeable loss of polymerized microtubules throughout the cells, and a significant change in cell shape was observed (Fig. 5d–f). At 3 and 10 μmol/l, there was a complete loss of microtubule network and an increase in prominent peripheral stress fibers. Cells were more contracted, and some even collapsed (Fig. 5g–i, 10 μmol/l only).

To determine whether the effect of ABT-751 on endothelial morphology was reversible, cells were washed

Table 2 MAP and HR measured before, and 0.5 and 1 h post-ABT-751 administration

	Time postdosing (h)					
	0	0.5	1	0	0.5	1
	MAP (mean ± SEM) (mmHg)			HR (Mean ± SEM) (beats/min)		
Vehicle	117.8 ± 4.7	113.2 ± 5.8	93.6 ± 5.4	403.4 ± 16.3	364.9 ± 18.9	351.5 ± 19.8
ABT-751	119.1 ± 5.5*	124.8 ± 6.3*	104.4 ± 7.2*	369.6 ± 14.8*	372.9 ± 14.3*	363.5 ± 11.7*

ABT-751 did not cause significant changes in either mean arterial pressure (MAP) or heart rate (HR) within 1 h after dosing, despite significant changes in tumor vascular function by ABT-751.
*$P > 0.2$ compared with vehicle group.

Fig. 5

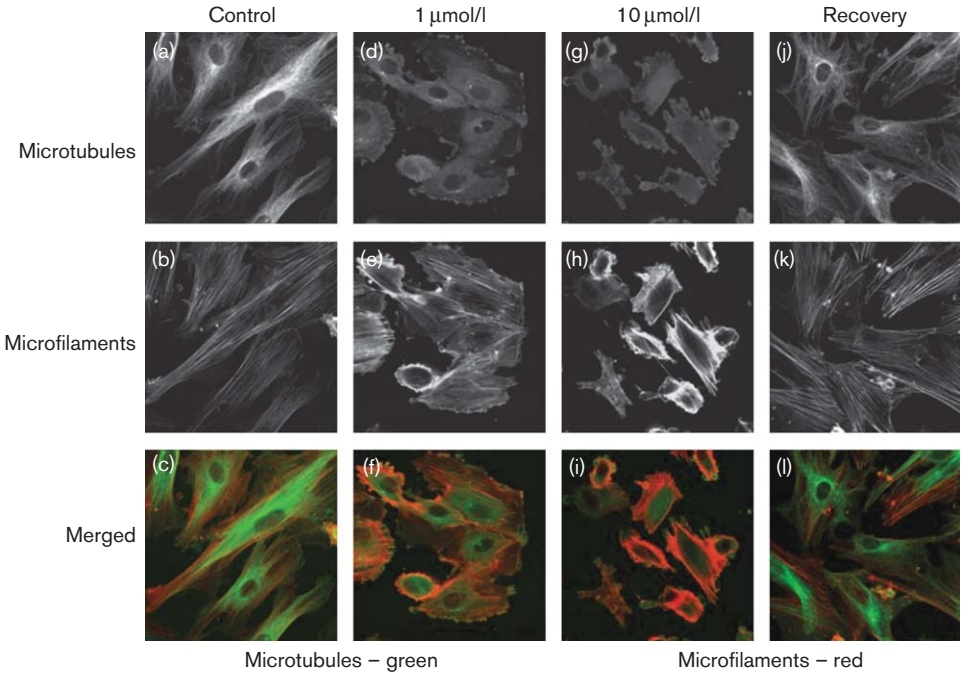

Effect of ABT-751 on endothelial cell morphology and cytoskeletal organization. Human microvascular endothelial cells were treated with ABT-751 for 1 h and either fixed immediately or allowed to recover for 5 h before fixing. Cells were stained for microtubules (a, d, g, and j) and microfilaments (b, e, h, and k). (a–c) Untreated controls, (d–f) cells treated with 1 μmol/l ABT-751, (g–i) cells treated with 10 μmol/l ABT-751, and (j–l) cells treated 1 h with 10 μmol/l ABT-751 followed by 5 h recovery. (c, f, i, and l) Merged images of microtubules (green) and microfilaments (red).

Table 3 Tumor NAF measured at 1 and 6 h after dosing with ABT-751

	Tumor NAF ± SD	
Treatment	1 h postdose	6 h postdose
Vehicle	0.20 ± 0.07	0.19 ± 0.15
ABT-751	0.12 ± 0.09	0.24 ± 0.11

There were no significant differences in necrotic area fraction (NAF) of the ABT-751 group compared with the vehicle group.

1 h after the treatment and allowed to recover for 5 h in drug-free medium. Cellular extension was noticeable at all treatment concentrations during 1-h recovery period. By 5 h, most of the cells were well extended at all compound levels. The cells had an extensive microtubule network and stress fibers along the body of the cells similar to untreated control cells. However, cell orientation was less organized than was observed in the controls (Fig. 5j–l, 10 μmol/l only). Drug treatment had no effect on endothelial cell survival as evaluated with propidium iodide staining at the end of the 6 h period. These data suggest that at physiological concentrations, ABT-751 can reversibly alter the morphology of endothelial cells.

Histomorphometry

Along the periphery of the tumor were viable, hypercellular masses with higher vessel density. The central portion of the tumor presented different degrees of necrosis. The tumor NAF from tumors taken 1 and 6 h post-ABT-751 is shown in Table 3. Although there was a trend toward an increase in average NAF from 1 to 6 h in the ABT-751-treated group, and a marginal increase of NAF in ABT-751-treated group versus the vehicle control group at 6 h, the difference in mean NAF between the groups was not statistically significant.

Discussion

This study shows that a single treatment of ABT-751 at a dose 10 times lower than the MTD (approximately 300 mg/kg) selectively disrupts tumor vascular function as determined using DCE-MRI. Specifically, ABT-751 causes a profound but acute reduction in the perfusion indices S_M and IAUC of tumor but not of normal muscle. Furthermore, this vascular activity was a transient event, since 6 h after compound administration, tumor perfusion indices largely recovered and showed no significant differences from those measured in vehicle-treated rats.

These observations are consistent with our earlier findings using an isolated tumor model in rats, where we found a dose-dependent decrease in tumor blood flow and an increase in tumor vascular resistance after the treatment of ABT-751 [30]. One explanation for the

changes in tumor blood flow observed after the ABT-751 treatment may relate to a change in the morphology of endothelial cells. Blood vessels in tumors differ from those in normal tissues in that tumor vessels are disorganized, thin-walled, and contain a relatively high proportion of proliferating endothelial cells. Earlier studies have shown that VDAs can exploit these distinctive features of the tumor vasculature to affect blood flow in tumors [6,19,43]. For example, treatment with ZD6126 results in conformational changes in immature, proliferating, but not mature, nonproliferating endothelial cells *in vitro* and leads to endothelial cell contraction, blood vessel congestion, and consequently, tumor cell death *in vivo*. In this study, we used nonconfluent proliferating endothelial cells to better mimic the immature blood vasculature *in vivo*. ABT-751, at physiologically relevant levels, directly and reversibly affected endothelial cell morphology *in vitro*. Short incubation with ABT-751 did not affect cell viability, but caused a significant loss of peripheral microtubules that led to changes in cell shape. These effects were rapid, reversible, and correlated with the time-dependent vascular disruption observed *in vivo*, and thus supports the supposition that microtubule disruption of endothelial cells may be responsible, in part, for the fast-acting, dramatic decreases in tumor perfusion by VDAs [6,17,19].

Besides its antimitotic function, our results show that ABT-751 also has antivascular properties. Knowing the effective drug exposures required for each function, ABT-751 has the potential to be useful in different therapeutic regimens, where the agent can function as an antimitotic agent to directly attack tumor cells and/or as an antivascular agent to diminish tumor blood flow. In this study, the plasma concentration measured at 1 h after ABT-751 administration averaged 2.1 μmol/l, when a significant reduction in S_M and IAUC was observed. In a study reported by Segreti *et al.* [30], where multiple doses were tested, ABT-751 induced vascular disruption at doses of 10 and 30 mg/kg, but not at 3 mg/kg. The corresponding plasma concentrations of ABT-751 measured at 2 h after dosing at 10 and 30 mg/kg were 0.4 and 1.2 μmol/l, respectively; tumor vascular resistance remained elevated in the animals treated at 30 mg/kg but returned to baseline in animals treated at 10 mg/kg [30]. Taken together, it is estimated that the minimum plasma concentration required for antivascular effects by ABT-751 is in the range of 1.0–2.0 μmol/l. In contrast, to have significant antitumor effect, the efficacious concentration determined in preclinical tumor models is in the range of 1.0–4.0 μmol/l, and required prolonged compound exposure (>12 h) to produce significant inhibition of cell proliferation [26,44]. In summary, ABT-751 at a plasma concentration greater than 1.0 μmol/l, if maintained for an extended time, may produce simultaneous antimitotic and antivascular effects, whereas a short exposure to ABT-751 at approximately 1–2 μmol/l may selectively disrupt tumor vascular function without being directly toxic to tumor or normal cells.

Results from phase I clinical trials in patients with solid tumors showed that ABT-751 is an orally bioavailable compound with favorable absorption and clearance [25–27,45,46]. With single (approximately 300 mg/m^2) or 5-day repeated (approximately 220 mg/m^2) oral dosing regimen, peak plasma concentrations achieved were greater than 50 μmol/l, a concentration well above the predicted efficacious level required for antivascular and antitumor effects in preclinical models [21]. In more recent phase I trials using a multiple dosing schedule (7 consecutive daily dosing, every 3 weeks), plasma concentrations (both maximum concentration, C_{max} and minimum concentration, C_{min}) also achieved predicted efficacious levels at tolerable doses [26,45]. Unlike other agents of the same class, such as combretastatin A-4 and AVE8062, which are under development specifically for their vascular-mediated antitumor benefit, ABT-751 is being developed as an antimitotic agent. Thus, current clinical trials have focused on dosing regimens optimal for efficacy directly against tumor cells through antimitosis. In a recent phase II clinical trial in patients with advanced taxane-refractory non-small cell lung carcinoma, single-agent treatment with ABT-751 at 200 mg daily for 21 days followed by 7 days off was well tolerated and achieved comparable efficacy with current treatments approved for second-line therapy [47]. These results warrant further evaluation of this compound in combination treatment for enhanced treatment benefits.

Interestingly, there are two important characteristics of VDAs that should be considered. First, these agents may provide a means to achieve dynamic control of tumor blood flow, a function that is desired in many adjuvant therapies to potentiate primary tumor damage [48]. It has been shown in preclinical experiments that enhanced antitumor effects were achieved by VDAs when combined with radiation, antiangiogenic therapy, or with other cytotoxic agents [49–55]. As only a short exposure is required for antivascular effects with ABT-751, when combined with other treatment approaches, ABT-751 may enhance the treatment efficacy with a favorable tolerability. Second, because of this fast-acting, dramatic disruption of tumor vessel function, when VDAs are administered with frequent dosing or in combination with other treatments, the disrupted tumor vessel function may compromise drug delivery of subsequent doses or the combined treatments to the tumor. Thus, the identification of optimal time window between doses and the sequence of compound administration are important for treatment outcome and should be carefully designed. Based on our observations, ABT-751 produced transient tumor vessel disruption at 1–6 h after dosing. Vascular

consequences on compound delivery should thus not be a concern with once a day or twice a day dosing in a single-agent treatment regimen.

In conclusion, ABT-751 is a novel tubulin-binding agent that produces potent tumor-selective antivascular effects at tolerable doses in a preclinical model. The favorable bioavailability and safety profile achieved in human cancer trials offer opportunities for clinical development of ABT-751 as an antimitotic agent and/or a VDA.

Acknowledgements

The authors thank Ms Joy L. Bauch for the pharmacokinetics analysis and Dr Sabu Kuruvilla and Dr Jane A. Fagerland for their help with histological analysis.

References

1 Dhanabal M, Jeffers M, Larochelle WJ. Anti-angiogenic therapy as a cancer treatment paradigm. *Curr Med Chem Anticancer Agents* 2005; **5**:115–130.
2 Petersen I. Antiangiogenesis, anti-VEGF(R) and outlook. *Recent Results Cancer Res* 2007; **176**:189–199.
3 Harris AL. Antiangiogenesis for cancer therapy. *Lancet* 1997; **349** (**Suppl 2**):SII13–SII15.
4 Schlaeppi JM, Wood JM. Targeting vascular endothelial growth factor (VEGF) for anti-tumor therapy, by anti-VEGF neutralizing monoclonal antibodies or by VEGF receptor tyrosine-kinase inhibitors. *Cancer Metastasis Rev* 1999; **18**:473–481.
5 Wood JM, Bold G, Buchdunger E, Cozens R, Ferrari S, Frei J, *et al*. PTK787/ZK 222584, a novel and potent inhibitor of vascular endothelial growth factor receptor tyrosine kinases, impairs vascular endothelial growth factor-induced responses and tumor growth after oral administration. *Cancer Res* 2000; **60**:2178–2189.
6 Kanthou C, Tozer GM. Tumour targeting by microtubule-depolymerizing vascular disrupting agents. *Expert Opin Ther Targets* 2007; **11**:1443–1457.
7 Chaplin DJ, Horsman MR, Siemann DW. Current development status of small-molecule vascular disrupting agents. *Curr Opin Investig Drugs* 2006; **7**:522–528.
8 Chaplin DJ, Pettit GR, Parkins CS, Hill SA. Antivascular approaches to solid tumour therapy: evaluation of tubulin binding agents. *Br J Cancer Suppl* 1996; **27**:S86–S88.
9 Thorpe PE. Vascular targeting agents as cancer therapeutics. *Clin Cancer Res* 2004; **10**:415–427.
10 Siemann DW, Chaplin DJ, Horsman MR. Vascular-targeting therapies for treatment of malignant disease. *Cancer* 2004; **100**:2491–2499.
11 Warren B. The vascular morphology of tumors. In: Peterson HI. *Tumor blood circulation*. Boca Raton: CRC Press; 1979. pp. 1–47.
12 Eberhard A, Kahlert S, Goede V, Hemmerlein B, Plate KH, Augustin HG. Heterogeneity of angiogenesis and blood vessel maturation in human tumors: implications for antiangiogenic tumor therapies. *Cancer Res* 2000; **60**:1388–1393.
13 Hill SA, Lonergan SJ, Denekamp J, Chaplin DJ. Vinca alkaloids: anti-vascular effects in a murine tumour. *Eur J Cancer* 1993; **29A**:1320–1324.
14 Baguley BC, Holdaway KM, Thomsen LL, Zhuang L, Zwi LJ. Inhibition of growth of colon 38 adenocarcinoma by vinblastine and colchicine: evidence for a vascular mechanism. *Eur J Cancer* 1991; **27**:482–487.
15 West CM, Price P. Combretastatin A4 phosphate. *Anticancer Drugs* 2004; **15**:179–187.
16 Chaplin DJ, Hill SA. The development of combretastatin A4 phosphate as a vascular targeting agent. *Int J Radiat Oncol Biol Phys* 2002; **54**:1491–1496.
17 Tozer GM, Prise VE, Wilson J, Locke RJ, Vojnovic B, Stratford MR, *et al*. Combretastatin A-4 phosphate as a tumor vascular-targeting agent: early effects in tumors and normal tissues. *Cancer Res* 1999; **59**:1626–1634.
18 Micheletti G, Poli M, Borsotti P, Martinelli M, Imberti B, Taraboletti G, *et al*. Vascular-targeting activity of ZD6126, a novel tubulin-binding agent. *Cancer Res* 2003; **63**:1534–1537.
19 Davis PD, Dougherty GJ, Blakey DC, Galbraith SM, Tozer GM, Holder AL, *et al*. ZD6126: a novel vascular-targeting agent that causes selective destruction of tumor vasculature. *Cancer Res* 2002; **62**:7247–7253.
20 Hori K, Saito S. Microvascular mechanisms by which the combretastatin A-4 derivative AC7700 (AVE8062) induces tumour blood flow stasis. *Br J Cancer* 2003; **89**:1334–1344.
21 Yoshimatsu K, Yamaguchi A, Yoshino H, Koyanagi N, Kitoh K. Mechanism of action of E7010, an orally active sulfonamide antitumor agent: inhibition of mitosis by binding to the colchicine site of tubulin. *Cancer Res* 1997; **57**:3208–3213.
22 Koyanagi N, Nagasu T, Fujita F, Watanabe T, Tsukahara K, Funahashi Y, *et al*. In vivo tumor growth inhibition produced by a novel sulfonamide, E7010, against rodent and human tumors. *Cancer Res* 1994; **54**:1702–1706.
23 Funahashi Y, Koyanagi N, Kitoh K. Effect of E7010 on liver metastasis and life span of syngeneic C57BL/6 mice bearing orthotopically transplanted murine colon 38 tumor. *Cancer Chemother Pharmacol* 2001; **47**:179–184.
24 Morton CL, Favours EG, Mercer KS, Boltz CR, Crumpton JC, Tucker C, *et al*. Evaluation of ABT-751 against childhood cancer models in vivo. *Invest New Drugs* 2007; **25**:285–295.
25 Yee KW, Hagey A, Verstovsek S, Cortes J, Garcia-Manero G, O'Brien SM, *et al*. Phase 1 study of ABT-751, a novel microtubule inhibitor, in patients with refractory hematologic malignancies. *Clin Cancer Res* 2005; **11**:6615–6624.
26 Hande KR, Hagey A, Berlin J, Cai Y, Meek K, Kobayashi H, *et al*. The pharmacokinetics and safety of ABT-751, a novel, orally bioavailable sulfonamide antimitotic agent: results of a phase 1 study. *Clin Cancer Res* 2006; **12**:2834–2840.
27 Yamamoto K, Noda K, Yoshimura A, Fukuoka M, Furuse K, Niitani H. Phase I study of E7010. *Cancer Chemother Pharmacol* 1998; **42**:127–134.
28 Iwamoto Y, Nishio K, Fukumoto H, Yoshimatsu K, Yamakido M, Saijo N. Preferential binding of E7010 to murine beta 3-tubulin and decreased beta 3-tubulin in E7010-resistant cell lines. *Jpn J Cancer Res* 1998; **89**:954–962.
29 Nihei Y, Suzuki M, Okano A, Tsuji T, Akiyama Y, Tsuruo T, *et al*. Evaluation of antivascular and antimitotic effects of tubulin binding agents in solid tumor therapy. *Jpn J Cancer Res* 1999; **90**:1387–1395.
30 Segreti JA, Polakowski JS, Koch KA, Marsh KC, Bauch JL, Rosenberg SH, *et al*. Tumor selective antivascular effects of the novel antimitotic compound ABT-751: an in vivo rat regional hemodynamic study. *Cancer Chemother Pharmacol* 2004; **54**:273–281.
31 Luo Y, Hradil VP, Mohning KM, Nuss ME, Sham HL, Rosenberg SH, *et al*. Evaluation of anti-vascular effects of ABT-751 and A-318315 using dynamic contrast enhanced MRI (DCE-MRI). *Proc Int Soc Magn Reson Med* 2002; **3**:2140.
32 O'Connor JP, Jackson A, Parker GJ, Jayson GC. DCE-MRI biomarkers in the clinical evaluation of antiangiogenic and vascular disrupting agents. *Br J Cancer* 2007; **96**:189–195.
33 Robinson SP, McIntyre DJ, Checkley D, Tessier JJ, Howe FA, Griffiths JR, *et al*. Tumour dose response to the antivascular agent ZD6126 assessed by magnetic resonance imaging. *Br J Cancer* 2003; **88**:1592–1597.
34 Maxwell RJ, Wilson J, Prise VE, Vojnovic B, Rustin GJ, Lodge MA, *et al*. Evaluation of the anti-vascular effects of combretastatin in rodent tumours by dynamic contrast enhanced MRI. *NMR Biomed* 2002; **15**:89–98.
35 McIntyre DJ, Robinson SP, Howe FA, Griffiths JR, Ryan AJ, Blakey DC, *et al*. Single dose of the antivascular agent, ZD6126 (N-acetylcolchinol-O-phosphate), reduces perfusion for at least 96 h in the GH3 prolactinoma rat tumor model. *Neoplasia* 2004; **6**:150–157.
36 Stevenson JP, Rosen M, Sun W, Gallagher M, Haller DG, Vaughn D, *et al*. Phase I trial of the antivascular agent combretastatin A4 phosphate on a 5-day schedule to patients with cancer: magnetic resonance imaging evidence for altered tumor blood flow. *J Clin Oncol* 2003; **21**:4428–4438.
37 Tofts PS. Modeling tracer kinetics in dynamic Gd-DTPA MR imaging. *J Magn Reson Imaging* 1997; **7**:91–101.
38 Evelhoch JL, LoRusso PM, He Z, DelProposto Z, Polin L, Corbett TH, *et al*. Magnetic resonance imaging measurements of the response of murine and human tumors to the vascular-targeting agent ZD6126. *Clin Cancer Res* 2004; **10**:3650–3657.
39 Wilke N, Jerosch-Herold M, Wang Y, Huang Y, Christensen BV, Stillman AE, *et al*. Myocardial perfusion reserve: assessment with multisection, quantitative, first-pass MR imaging. *Radiology* 1997; **204**:373–384.
40 Luo Y, Mohning KM, Hradil VP, Wessale JL, Segreti JA, Nuss ME, *et al*. Evaluation of tissue perfusion in a rat model of hind-limb muscle ischemia using dynamic contrast-enhanced magnetic resonance imaging. *J Magn Reson Imaging* 2002; **16**:277–283.
41 Verstraete KL, Van der Woude HJ, Hogendoorn PC, De-Deene Y, Kunnen M, Bloem JL. Dynamic contrast-enhanced MR imaging of musculoskeletal

tumors: basic principles and clinical applications. *J Magn Reson Imaging* 1996; **6**:311–321.
42 Chen J, Wu W, Tahir SK, Kroeger PE, Rosenberg SH, Cowsert LM, *et al.* Down-regulation of survivin by antisense oligonucleotides increases apoptosis, inhibits cytokinesis and anchorage-independent growth. *Neoplasia* 2000; **2**:235–241.
43 Tozer GM, Akerman S, Cross NA, Barber PR, Bjorndahl MA, Greco O, *et al.* Blood vessel maturation and response to vascular-disrupting therapy in single vascular endothelial growth factor-A isoform-producing tumors. *Cancer Res* 2008; **68**:2301–2311.
44 Yokoi A, Kuromitsu J, Kawai T, Nagasu T, Sugi NH, Yoshimatsu K, *et al.* Profiling novel sulfonamide antitumor agents with cell-based phenotypic screens and array-based gene expression analysis. *Mol Cancer Ther* 2002; **1**:275–286.
45 Fox E, Maris JM, Widemann BC, Meek K, Goodwin A, Goodspeed W, *et al.* A phase 1 study of ABT-751, an orally bioavailable tubulin inhibitor, administered daily for 7 days every 21 days in pediatric patients with solid tumors. *Clin Cancer Res* 2006; **12**:4882–4887.
46 Fox E, Maris JM, Widemann BC, Goodspeed W, Goodwin A, Kromplewski M, *et al.* A phase I study of ABT-751, an orally bioavailable tubulin inhibitor, administered daily for 21 days every 28 days in pediatric patients with solid tumors. *Clin Cancer Res* 2008; **14**:1111–1115.
47 Mauer AM, Cohen EE, Ma PC, Kozloff MF, Schwartzberg L, Coates AI, *et al.* A phase II study of ABT-751 in patients with advanced non-small cell lung cancer. *J Thorac Oncol* 2008; **3**:631–636.
48 Horsman MR, Chaplin DJ, Overgaard J. The use of blood flow modifiers to improve the treatment response of solid tumors. *Radiother Oncol* 1991; **20** (**Suppl 1**):47–52.
49 Jorgensen TJ, Tian H, Joseph IB, Menon K, Frost D. Chemosensitization and radiosensitization of human lung and colon cancers by antimitotic agent, ABT-751, in athymic murine xenograft models of subcutaneous tumor growth. *Cancer Chemother Pharmacol* 2007; **59**:725–732.
50 Hori K, Furumoto S, Kubota K. Tumor blood flow interruption after radiotherapy strongly inhibits tumor regrowth. *Cancer Sci* 2008; **99**:1485–1491.
51 Goto H, Yano S, Matsumori Y, Ogawa H, Blakey DC, Sone S. Sensitization of tumor-associated endothelial cell apoptosis by the novel vascular-targeting agent ZD6126 in combination with cisplatin. *Clin Cancer Res* 2004; **10**:7671–7676.
52 Hokland SL, Horsman MR. The new vascular disrupting agent combretastatin-A1-disodium-phosphate (OXi4503) enhances tumour response to mild hyperthermia and thermoradiosensitization. *Int J Hyperthermia* 2007; **23**:599–606.
53 Chaplin DJ, Pettit GR, Hill SA. Anti-vascular approaches to solid tumour therapy: evaluation of combretastatin A4 phosphate. *Anticancer Res* 1999; **19**:189–195.
54 Siim BG, Lee AE, Shalal-Zwain S, Pruijn FB, McKeage MJ, Wilson WR. Marked potentiation of the antitumour activity of chemotherapeutic drugs by the antivascular agent 5,6-dimethylxanthenone-4-acetic acid (DMXAA). *Cancer Chemother Pharmacol* 2003; **51**:43–52.
55 Soltau J, Drevs J. ZD-6126 AstraZeneca. *I Drugs* 2004; **7**:380–387.